International Journal of Engineering Research and Development
e-ISSN: 2278-067X, **p**-ISSN : 2278-800X, www.ijerd.com
Volume 5, Issue 3 (December 2012), PP. 68-86

Matlab Based Static I-V Characteristics of Optically Controlled GaAs MESFET'S

Sanjay.C.Patil[1], B.K.Mishra[2]
[1] (Research Scholar at NMIMS (MUMBAI)**,** Parshvanath College of Engineering, THANE (W), MUMBAI, 400601 INDIA
[3]Thakur College of Engineering and Technology, Kandivali (E) MUMBAI, 400101 INDIA

Abstract: - Optoelectronic is one of the thrust areas for the recent research activity. One of the key components of the optoelectronic family is photo detector to be widely used in broadband communication, optical computing, optical transformer, optical control etc. Result's that theoretical predicted for device and using MATLAB are quite similar A new analytical model for the static I-V characteristics of GaAs MESFET's under optically controlled conditions in both linear and saturation region is presented in this paper. The novelty of the model lies in characterizing both photovoltaic (external, internal) and photoconductive effects. Deep level traps in the semi insulating GaAs substrate are also included in this model. Finally, effect of backgate voltage on I-V characteristics is explained analytically for the first time in literature. Small signal parameters of GaAs MESFET are derived under both dark and illuminated conditions.

Keywords*:* - Optically controlled GaAs MESFET, photo voltage, deep level traps, backgating, and channel length modulation**.**

I. INTRODUCTION

Optically controlled GaAs MESFET (OPFET) is the considered key device used for the design of photo-detector [1-3]. It is experimentally established fact that optical radiation incident on the transparent or semitransparent gate of the device is used to control the microwave characteristics of the OPFET [4-5]. It has also been investigated that many of the microwave characteristics of GaAs MESFET like resonant frequency, transit time etc., can be controlled by controlling the internal gate-source and gate-drain capacitances of the device [6-7]. Here it is worth mention that the level of incident illumination can change the charge distribution under the gate that determines the internal capacitances of the GaAs MESFET. Therefore the internal capacitances of GaAs MESFET can also be controlled by the incident illumination.

Optical control of microwave devices and circuits has been a fertile area of research for the past two decades [1]. In particular, optically controlled GaAs MESFET's (OPFET's) have drawn considerable attention as potential active devices in photo detector as well as in OEIC's [2-9]. Optical control has many advantages for complex microwave systems such as size reduction, signal isolation, large bandwidth and immunity to electromagnetic interference. With such numerous advantages many potential application like optically controlled amplifiers, oscillators, Light Amplifying Optical Switch (LAOS) and phase shifters, to name a few, become feasible [3-5, 7-9]. The possibility of making use of optical sensitivity of MESFET to form an additional signal input port justifies an increased interest in physical mechanism which occurs when MESFET is illuminated. When photonic MMIC is designed in such a way as to involve the optical phenomenon mentioned above, the circuit designer is immediately aware of the necessity of a good model with all major effects considered. Several researchers experimentally showed that gain, drain current and S-parameters of GaAs MESFET can be controlled by varying incident light on the device in the same manner as varying the gate bias voltage [4, 7-9].

Modeling of I-V characteristics of optically controlled GaAs MESFET has been carried out over the years by several researchers. Salles [7] reported an over simplified analytical model for the I-V characteristics of GaAs MESFET under optically controlled conditions and estimated changes in MESFET small signal parameters due to illumination. Simons [10] derived analytical expressions for I-V characteristics of different types of FET configurations under optical illumination on the devices. He also computed variations in FET small signal parameters such as transconductance, channel conductance with illumination. Singh *et al.* [11] reported an analytical model for the drain-source current of optically controlled GaAs MESFET. Chakrabarti *et al.* [12] presented an analytical model for the photo-dependent I-V characteristics of GaAs MESFET and explained their results by means of both the excess photo-generated carriers in the depletion region and the photo voltage developed across the Schottky junction. Since, excess holes in the depletion region due to the

illumination develop photo voltage across the Schottky junction, inclusion of both these effects (photo-generated excess carriers and photo-induced gate voltage) simultaneously seems to be ambiguous. Further, they also ignored the effect of excess photo-generated carriers in the neutral region. Moreover, the resultant model was very complex as compared to Singh *et al.* [11]. Kawasaki *et al.* [4] demonstrated an illuminated FET model by including an illumination intensity parameter in the *modified Statz* model with a large number of unknown fitting parameters to be extracted either from extensive experimental or from simulation results. Some two-dimensional numerical models of optically controlled GaAs MESFET's are also reported in the literature [13] In this paper we present an analytical modeling of static I-V characteristics of optically controlled GaAs MESFET's in both linear and saturation regions of operation. A comprehensive analytical characterization of photo induced voltages (both internal and external) and photoconductive current in the channel is presented. Deep level traps in the semi insulating substrate as well as in the active layer are considered through which the important effect, backgating is analytically modeled for the first time in the literature under illuminated conditions. In linear region gradual channel approximation is used and in saturation region channel length modulation is considered as a source of finite output conductance. Later, small signal parameters of GaAs MESFET under optically controlled conditions are derived from the static I-V characteristics.

II. THEORETICAL MODEL

The schematic structure of a non-self-aligned GaAs MESFET is shown in Fig 1. Gate area of the device is illuminated with monochromatic light of energy greater than or equal to the band gap energy of GaAs. The metal gate used for the Schottky contact is assumed to be transparent/ semitransparent to the incident light [5, 11-12]. The substrate of the device is assumed to be an undoped high-pure LEC semi-insulating GaAs material. The active channel region of the device is an n-GaAs layer which can be obtained by ion implanting Si into the SI substrate.

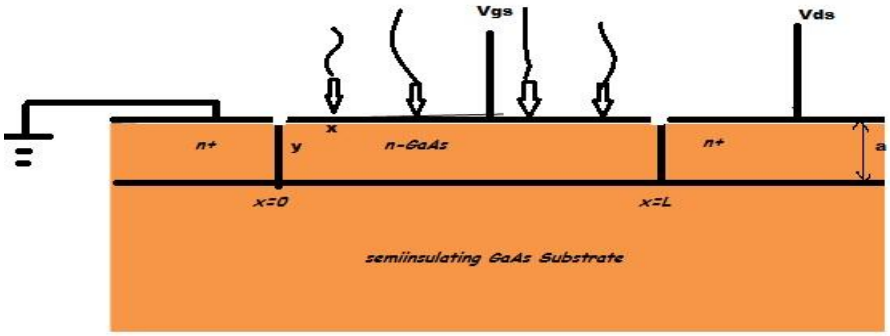

Fig.1. schematic of Gaas MESFET

In Fig. 1, the depletion region at y=0,is a conventional depletion region of Schottky gate and the other depletion region is formed at the channel-substrate interface (at *y*=a) due to the deep level traps in the SI substrate [15, 18]. We call the above two depletion regions as *front* and *back* depletion regions respectively. The widths of these depletion regions are strongly dependent on the substrate properties as well as on the backgate voltage which in turn effects current flowing through the channel. Thus, substrate induced effects are crucial in determining I-V characteristics of the device.

1. Modeling of the Deep Level Traps and Backgating Effects

One method for rendering undoped GaAs wafers semi-insulating is through the careful control of melt stoichiometry during LEC growth. It has been shown that a slight excess of As in the melt favors the formation of EL2 deep donors that compensates residual shallow acceptors (C from B_2O_3 encapsulant) and shallow donors (S or Si) [15]. The probability of an EL2 level to be occupied by an electron in the SI-substrate under thermal equilibrium condition is given by the Fermi function [18].

$$f_{eql}(EL2) = \{1 + \frac{1}{g}\exp[\frac{(E_T - E_{fs})}{kT}]\}^{-1} \quad -(1)$$

Where E_T energy of the EL2 level E_{fs} is the Fermi energy level in the substrate bulk, $g = 2$ is the degeneracy factor of EL2.

The position of Fermi level in the substrate bulk can be obtained from charge neutrality condition in the substrat

$$N^{+}_{EL2,S} + N^{+}_{SD} - N^{-}_{SA} + p_{sub} - n_{sub} = 0 - (2)$$

where

$$N^{+}_{EL2,S} = N_{EL2}(1 - f_{eql}(EL2) = N_{EL2}\{1 + 2\exp[\frac{(E_{fs} - E_T}{kT}]\}^{-1}$$

is the density of ionized EL2 traps, n_{sub}, p_{sub} $N^{+}_{SD} \approx N_{SD}$ and $N^{-}_{SA} \approx N_{SA}$ are the free electron, hole, ionized shallow donor and ionized shallow acceptor concentrations in the bulk substrate under equilibrium condition respectively. Since n_{sub} and p_{sub} are negligibly small as compared to other ionized impurities of equation (2), we may write

$$E_c - E_{fs} \approx (E_c - E_T) - kT\ln(\frac{N_{EL2} + N_{SD} - N_{SA}}{2(N_{SA} - N_{SD})}) - (3)$$

Under steady-state non-equilibrium condition, the Fermi statistics described by Eqn (1) becomes invalid. In this case, the Fermi function can be given by

$$f_{non-eql}(EL_2) = \frac{e_p + nC_n}{e_p + ne_n + pC_p} - (4)$$

Where $C_p = \sigma_p v_{pth}$ $and C_n = \sigma_n v_{nth}$

Are the electron and hole capture coefficients σ_p and σ_n are the capture cross section of holes and electrons ;n and p are the electron and hole concentration under non-equilibrium conditions ; v_{pth} and v_{nth} are the thermal velocities of holes and electrons; e_p and e_n are the emission rates of holes and electrons from EL2 levels respectively

The formation of the back depletion region at the channel-substrate interface is due to the fact that some of the free electrons in the channel gain sufficient energy and enter into the substrate. These electrons are captured by the EL2 traps and a negative space charge region is created at the substrate side [15]. As a result, a depletion region is created at the backside of the channel. The negative charge density accumulated in the substrate can be determined as follows:

Since and n & p are negligible in the semi-insulating substrate, the concentration of neutral EL2 states in the substrate side near the channel-substrate (CS) interface under steady-state non-equilibrium condition is given by

$$N^{0}_{EL2} = (non-eql) = N_{EL2} f_{non\_eql}(EL2) \vdots n = p \approx 0$$

$$= N_{EL2}\left[\frac{e_p}{e_n + e_p}\right] - (5)$$

The concentration of negative charge in the substrate side of the CS junction is,is the density of occupied EL2 traps in the bulk substrate under thermal equilibrium condition.
Neglecting the free carrier concentrations in the depletion regions (i.e.0==*pn*), the concentration of ionized EL2 states in these depletion regions may be given by

$$N^{-}_{sub} = N^{0}_{EL2}(non-epl) - N^{0}_{EL2}(egl)$$

$$= \left\{N_{EL2}\left[\frac{e_p}{e_p + e_n}\right]\right\} - \left\{N_{EL2}\left\{1 + \frac{1}{2}\exp\left[\frac{(E_T E_{fs}}{kT}\right]\right\}^{-1}\right\} - (6)$$

Where

$$N^{0}_{EL2}(eql) = N_{EL2} f_{eql}(EL2)$$

$$= N_{EL2}\left\{1 + \frac{1}{2}\exp\left[\frac{(E_T - E_{fs})}{kT}\right]\right\}^{-1}$$

Is the density of occupied EL2 traps in the bulk substrate under thermal equilibrium condition.
Neglecting the free carrier concentrations in the depletion regions (i.e. n = p = 0), the concentration of ionized EL2 states in these depletion regions may be given by

$$N^{+D}_{EL2} \approx N_{EL2}\left(1 - f_{non\_eql}(EL2)\vdots_{n=p=0}\right) = N_{EL2}\left[\frac{e_p}{e_n + e_p}\right] - (7)$$

Assuming that N_d, N_{SD} and N_{SA} are fully ionized in the active layer .The total positive charge concentration in depletion layer becomes

$$N^{+}_{dep} = N_d + N_{SD} + N^{+D}_{EL2} - N_{SA} - (8)$$

A number of experimental and theoretical investigation reported in literature [16,19] suggest that There exists a backgating threshold voltage V_{thbg}, such that if the backgate voltage V_b is below certain threshold voltage V_{thbg}, substrate maintains high resistance with the backgate voltage drops primarily across the bulk substrate and has little effect on the channel thickness. But, when V_b exceeds V_{thbg} (i.e $V_{bg} > V_{thbg}$.), impact ionization of deep traps occurs and the semi insulating substrate transits from a state of high resistivity to low resistivity with the difference $V_{bg} - V_{thbg}$ drops across the CS interface thus widening the back depletion region and

narrowing the channel. To include the effect of V_{bg}, voltage across the CS junction for $V_{ds} = 0$ is expressed in the following form

$$V_{ch-s} = \{V_{bics}; \quad V_{bg} \le V_{thbg}$$

$$\{V_{bics} + (V_{bg} - V_{thbg}); \; V_{bg} > V_{thbg} \quad -(9)$$

Where V_{bics} is the built-in potential across the channel-substrate junction. Note that the absolute value of the substrate bias V_{bg} is assumed in Eqn (9). Here we have considered V_{thbg} as a parameter without going through details of modeling, details of exact modeling V_{thbg} can be found elsewhere [19].

We can model the additional voltage $f(V_{bg})$ (say) added to the gate as

$$f(V_{bg}) = \{0; \vdots V_{bg} \vdots \le V_{thbg}$$

$$= \{\alpha_1 (\vdots V_{bg} \vdots - V_{thbg}) + \alpha_2 (\vdots V_{bg} \vdots - V_{thbg})^2; \vdots V_{bg} \vdots > V_{thbg} \quad -(10)$$

the height of front depletion region at a distance x below the gate including V_{bg} is

$$h_{bg}^{f}(x) = \sqrt{\frac{2\varepsilon_s}{qN_{dep}^{+}}(V_{bi} - V_{gs} + f(V_{bg}) + V(x)} \quad -(11)$$

Where ε_s is permittivity of GaAs, V_{bi} is built-in potential across Schottky junction and $V(x)$ is the channel potential at any distance x measured with respect to the source.
Similarly, the height of back depletion region measured from channel-substrate interface(y=a) including backgating can be obtained by solving one dimensional Poisson's equation with appropriate boundary conditions [19]

$$h_{bg}^{b}(x) = \sqrt{\frac{2\varepsilon_s}{qN_{dep}^{+}}\left\{\frac{N_{sub}^{-}}{N_{dep}^{+} + N_{sub}^{-}}\right\}(V_{ch-s} + V(x))} \quad -(12)$$

Now ,the pinch-off voltage of the device may be written as

$$V_{po} = \frac{qN_{dep}^{+}}{2\varepsilon_s}\left(a - h_{bg}^{b}(L) \vdots V_{ds=0}\right)^2$$

$$= \frac{qN_{dep}^{+}}{2\varepsilon_s}\left[a - \sqrt{\frac{2\varepsilon_s V_{ch-s}}{qN_{dep}^{+}}\left\{\frac{N_{sub}^{-}}{N_{dep}^{+} + N_{sub}^{-}}\right\}}\right]^2 \quad -(13)$$

Threshold voltage of the MESFET V_{th} including backgating is

$$V_{th} = (V_{bi} + f(V_{bg})) - \left\{\frac{qN_{dep}^{+}}{2\varepsilon_s}\left[a - \sqrt{\frac{2\varepsilon_s V_{ch-s}}{qN_{dep}^{+}}\left\{\frac{N_{sub}^{-}}{N_{dep}^{+} + N_{sub}^{-}}\right\}}\right]^2\right\} - (14)$$

It is noted that for $N_{EL2} = N_{SD} = N_{SA} = 0$ and $V_{bg} = 0$ the thresh hold voltage equals to $V_{bg} - \frac{qN_d a^2}{2\varepsilon_s}$ which is the same as that of the conventional MESFET's

2. Modeling of Photovoltaic Effects

Let ϕ_0 be the incident photon flux density (i.e. number of photons per unit area per second) at y=0. Now ϕ_0 can be expressed in terms of input optical power as [12]

$$\phi_0 = \frac{(1 - R_m)(1 - R_s)P_{in}}{h\nu ZL} \quad -(15)$$

where P_{in} is the incident optical power, h is the Planck's constant, ν is the frequency of incident light, Z is the width of the gate-metal R_m and R_s are the reflection coefficients for normal incidence at metal surface and metal-semiconductor interface, respectively.

Since optical transmission through gate depends on thickness of gate metallization, the metal used for Schottky contact (such as gold) should be made sufficiently thin (~100 Å) to achieve higher transmittance up to 90-95% [5] at the cost of lower unity-gain frequency and higher noise figure. More recently some alternate materials are suggested such as Indium Tin Oxide (ITO) and Al or Ga doped ZnO [22-23]. These thin films are highly degenerate n-type semiconductors with low resistivity. Being wide band gap materials, these are transparent to visible light with transmittance up to 90%in the operating wavelength range500nm-900nm and form good Schottky contact with GaAs [22]. However, we have considered a semi-transparent/transparent gate with transmittance as a parameter (which can be determined by R_m and R_s as defined in Eqn 15) for different metals used for the Schottky contact. When GaAs MESFET is illuminated with optical radiation on the gate

area, absorption of photons takes place in the active channel region as well as in the substrate region of the device. The absorption of light results in the generation of electron-hole pairs in both depletion regions and in the neutral channel. Holes generated in gate-depletion and back-depletion regions are drifted out toward the metal and semi-insulating sides respectively due to the strong electric fields present in depletion regions. Photo-generated excess holes in the neutral channel region are diffused into the front and back depletion regions and are also finally swept out. Further, the photo-generated electrons in the substrate near the channel-substrate junction are also drifted into the active layer of the device. Thus, incident illumination results in two photocurrents: one flows from the active layer to the gate-metal and the other flows from active layer to the semi-insulating substrate. This results in developing photo-voltages across the Schottky junction (i.e. external photo voltage) [7] and the channel-substrate junction (i.e. internal photo voltage) [12]. However, due to the relatively complex structure of the depletion regions of the MESFET, we have assumed that the above induced photo-voltages are independent of the external biasing voltages, which is conformed by several experimental results [8, 13, 24].

i) Derivation of external photovoltage

Let $P^{f}(y)$ and $P^{ch}(y)$ be the photo-generated hole densities in the front depletion and neutral regions of the channel respectively. Assuming that the excess holes generated in the depletion region are swept out with saturation velocity towards the metal, $P^{f}(y)$ and $P^{ch}(y)$ may be obtained by solving the following steady state continuity equations [21]:

$$G_{opt} - \frac{p^{f}(y)}{\tau_{p}} - V_{p}\frac{\partial p^{f}(y)}{\partial y} + \left(D_{p}\frac{\partial^{2} p^{f}(y)}{\partial y^{2}}\right) = 0 \quad -(16)$$

$$D_{p}\frac{\partial^{2} p^{ch}(y)}{\partial y^{2}} + G_{opt} - \frac{(p^{ch} - p_{no})}{\tau_{p}} - = 0 \quad -(17)$$

Where is the $G_{opt} = \phi_{0}\alpha e^{-\alpha y}$ photo-generation rate of excess carriers, p_{no} is the hole concentration in the active layer under dark condition. τ_{p} $(= 1/\sigma_{p} V_{pth} N_{EL2}$ [18], V_{p} and D_{p} are the recombination lifetime, saturation velocity and diffusion coefficient of holes respectively. Note that the last term in the left hand side of Eqn (16) has been intentionally introduced to represent the diffusion of excess holes from bulk towards semiconductor-metal interface to include the surface recombination effect at that interface.
We may solve Eqn (16) using the following boundary conditions [21]:

$$p^{f}(y = h_{o}^{f}) = 0, D_{p}\left.\frac{\partial p^{f}(y)}{\partial y}\right|_{y=0} = S_{pm} p^{f}(0) \quad -(18)$$

Where S_{pm} $(= \sigma_p V_{pth} N_{st})$ is the surface recombination velocity of holes at y=0 with surface state density as N_{st} $(\approx 1X10^{12}\ cm^{-2})$ [18] and $h_o^f = \sqrt{\frac{2\varepsilon_s}{qN^+_{dep}} V_{bi}}$ is the height of schottky depletion region With no external bias.

First boundary condition of Eqn (18) states that excess hole concentration at depletion edge is very small due to the strong fields in the depletion region [21] where as second boundary condition represents the diffusion of excess holes towards the surface and eventual recombination at y=0

Now the photocurrent due to the excess holes generated in the front depletion region is

$$J_{dep}^{f}(y)\Big|_{y=0} = qV_p\, p^{f}(y)\Big|_{y=0} - qD_p \frac{\partial p^{f}(y)}{\partial y}\Big|_{y=0} = qV_p\, p^{f}(0) - qS_{pm}\, p^{f}(0) - (19)$$

The diffusion current component of excess holes in neutral region can be obtained by solving Eqn (17) with the following boundary conditions [21]

$$(p^{ch}_{no} - p_{no})\Big|_{y=h_o^f} \approx 0$$

$$(p^{ch}_{no} - p_{no})\Big|_{y=a-h_o^b} \approx 0 - (20)$$

Where $h_o^b = \sqrt{\frac{2\varepsilon_s}{qN^+_{dep}} \left(\frac{N^-_{sub}}{N^+_{dep} + N^-_{sub}}\right) V_{bics}}$ is back depletion width from y=0 into the channel due to the channel- substrate junction under no bias conditions. From Eqn (17), excess hole density in the neutral channel due to illumination is given by

$$p^{ch}(y) - p_{no} = \frac{\alpha\phi_0 \tau_p}{\alpha^2 L_p^2 - 1}\left[\frac{e^{-b_o^f}}{\xi}\sinh\left(\frac{y-h_o^f}{L_p}\right) - \frac{e^{-\alpha(a-h_o^b)}}{\xi}\sinh\left(\frac{y-(a-h_o^b)}{L_p}\right) - e^{-\alpha y}\right] - (21)$$

Where $\xi = \sinh\left[\frac{h_o^f - (a-h_o^b)}{L_p}\right]$ and $L_p = \sqrt{D_p \tau_p}$ is the diffusion length of holes

The resulting photocurrent density flowing from the active layer to the metal due to the diffusion of excess holes generated in the neutral region at depletion edge is

$$J_{diff}^{ch}(h_o^f) = -qD_p\left(\frac{\partial p^{ch}(y)}{\partial y}\right)\Bigg|_{y=h_o^f} \quad -(22)$$

Total photo current density flowing from semiconductor to metal at the gate junction is

$$J_{total} = \left|J_{depf}^{f}(0)\right| + \left|J_{diff}^{ch}(h_o^f)\right| \quad -(23)$$

The photo induced voltage developed across the Schottky junction is [5, 7, 12]

$$V_{op} = \frac{nkT}{q}\ln\left(1 + \frac{J_{total}}{J_s}\right) \quad -(24)$$

Where'n' is ideality factor, k is Boltzmann's constant, T is the operating temperature, q is electron charge and J_s is reverse saturation current density of the Schottky junction

ii) Derivation of internal photo voltage

Since the substrate-depletion region is much larger than that of the back depletion region [15] and the absorption coefficient of GaAs at wave length is $\lambda \approx 0.83\mu m$ it may be assumed that for the substrate heigh $D \approx 10\mu m >> 1/\alpha$, most of the absorption take place within the front, back and substrate-depletion regions. Hence optical absorption in the neutral region of the substrate may be neglected. The photo-voltage developed across the channel-substrate junction may be determined as below:

Photo-generated holes in the neutral channel are diffused into the back depletion region as well, diffusion current density at the edge of the back depletion region may be obtained in a similar manner as considered previously and may be written from Eqn (22)

$$J_{diff}^{ch}(a - h_o^b) = -qD_p\left.\frac{\partial p^{ch}(y)}{\partial y}\right|_{y=a-h_o^b} \quad -(25)$$

Let $p^b(y)$ be the excess photo generated hole density in the back depletion region. $p^b(y)$ may be obtained by solving

$$V_p\frac{\partial p^b}{\partial y} + \frac{p^b}{\tau_p} - G_{opt} = 0 \quad -(26)$$

Using boundary condition $p^b|_{y=a-h_o^b} \approx 0$ [21]. The solution of Eqn (26) is

$$p^{b}(y) = \frac{\alpha\phi_0 \tau_p}{\alpha V_p \tau_p - 1}\left\{\exp\left[-\left(a - h_o^{b}\right)\left(\alpha - \frac{1}{V_p \tau_p}\right) - \frac{y}{V_p \tau_p}\right] - \exp[-\alpha y]\right\} - (27)$$

The hole drift current density at channel-substrate boundary (y =a)is thus obtained as

$$J_{dr}^{b}(y = a) = qV_p\, p^{b}(y = a) - (28)$$

Now, the photo generated electrons in the substrate depletion region are also drifted towards the back depletion region resulting in a photocurrent component flowing from the channel to substrate side. The photo-generated electron density $n^{ss}(y)$ in the substrate-depletion region of channel-substrate junction may be obtained by solving [21]

$$V_n \frac{\partial n^{ss}}{\partial y} + \frac{n^{ss}}{\tau_n} - G_{opt} = 0 - (29)$$

Where V_n and τ_n $(= 1/\sigma_{nth} V_{EL2} N_n)$ are saturation velocity and recombination lifetime of electron in the substrate depletion region respectively .Using the boundary conditions $n^{ss} \vdots_{y = a + h_o^{ss} \approx 0}$ [21]

We may obtain

$$n^{ss}(y) = \frac{\alpha\phi_0 \tau_n}{\alpha V_n \tau_n - 1}\left\{\exp\left[-(a + h_o^{ss})\left(\alpha - \frac{1}{V_n \tau_n}\right) - \frac{y}{V_n \tau_n}\right] - \exp[-\alpha y]\right\} - (30)$$

Where $h_o^{ss} = \left(\frac{N_d}{N_{sub}}\right)\sqrt{\frac{2\varepsilon_s}{qN_{dep}^{+}}\left\{\frac{N_{sub}^{-}}{N_{dep}^{+} + N_{sub}^{-}}\right\}(V_{bics})}$ is the assumed

Height of the substrate-depletion region from $y=a$ under no bias condition. The electron drift current density at CS interface flowing from substrate into channel is

$$J_{dr}^{ss}(y = a) = qV_n\, n^{ss}(y = a) - (31)$$

Hence, the total photo current density flowing from the active layer to the substrate is

$$J_{total}^{ch-cs} = \vdots J_{diff}^{ch}(a - h_0^{b}) \vdots + \vdots J_{dr}^{b}(a) \vdots + \vdots J_{dr}^{ss}(a) \vdots - (32)$$

The photo voltage developed across this junction can be written as [12, 24],

$$V_{opt} = \frac{nkT}{q}\ln\left(1 + \frac{J_{ch-cs}^{total}}{J_{ch-cs}^{s}}\right) - (33)$$

Where is the reverse saturation current density at channel-substrate junction

iii) Photo conductive current

Along with photovoltaic effects photoconductive effects in active channel also manifests when the device is illuminated. Overall photo response of the device to optical illumination will be the superposition of both components considering one at a time. In the previous subsections we modeled photovoltaic effects without considering photoconductive effects. In this subsection we tried to quantify photoconductive effects.

Photo generated holes and electrons in the channel due to incident illumination contribute to the photoconductive current in the active region. Associated photoconductive current density can be expressed in terms of these carrier concentrations as

$$J_{pc} = q(n^{ch}V_n + p^{ch}V_p) - (34)$$

$$\frac{n^{ch}}{\tau_n} = \frac{p^{ch}}{\tau_p} - (35)$$

Interating ZJ_{pc} from $y = h_{bg}^{f}$ to $y = a - h_{bg}^{b}$

$$I_{pc} = \int_{y=h_{bg}^{f}}^{y=a-h_{bg}^{b}} ZJ_{pc}\,dy = Z\int_{y=h_{bg}^{f}}^{y=a-h_{bg}^{b}} P^{ch}q\left(\frac{n}{\tau_p}V_n + V_p\right)dy = Zq\left(\frac{n}{\tau_p}V_n + V_p\right)\int_{y=h_{bg}^{f}}^{y=a-h_{bg}^{b}} P^{ch}dy - (36)$$

in GaAs MESFET's the channel height is in sub-micron regime, diffusion length is several microns (typically 2-10μm) and the absorption coefficient is in the range $1 - 4X10^{6}/m$ for wavelengths 0.65-0.85-microns hence it is wise enough to assume . $\frac{a - h_{bg}^{f} - h_{bg}^{b}}{L_p} << 1$

Final simplified expression for photoconductive current after several approximations is

$$I_{pc} = 0.5Zq\frac{\alpha^2\phi_0\tau_p}{\alpha^2L^2 - 1}\left[\frac{n}{\tau_p}V_n + V_p\right]\left[a - h_{bg}^{f} - h_{bg}^{b}\right]^2 e^{-\alpha h_{bg}^{f}} - (37)$$

it can be seen that photoconductive current is a strong function of gate-source voltage and device parameters. As V_{gs} increases negatively effective channel opening $a - h_{bg}^{f} - h_{bg}^{b}$ decreases and photoconductive current also decreases. Due to square dependence of I_{pc} on effective channel opening magnitude of I_{pc} is generally in sub- microampere range

3. I-V Characteristics of GaAs MESFET under Illumination

De Salles [7] has shown experimentally that if a high resistance ($\geq k50\ \Omega$) is connected at the gate biasing circuit, photo-voltage developed across Schottky junction is superimposed on gate voltage. The effective gate-source bias under illumination becomes

$$V_{opgs} \approx V_{gs} + V_{op} \quad -(38)$$

Similarly, the photo-voltage developed across the channel-substrate junction will change the built-in potential across the junction [24]. It was also confirmed by 2-D numerical simulations [13]. The effective built-in potential under illuminated condition will be

$$V_{opbi} \approx V_{bics} + V_{opcs} \quad -(39)$$

Drain-source current of GaAs MESFET under illuminated condition will be the superposition of both photovoltaic and photoconductive effects

$$I_{ds} = I_{pv} + I_{pc} \quad -(40)$$

Where I_{ds} is final drain-source current, I_{pv} is drain-source current including photovoltaic effect only and I_{pc} is the photoconductive current in the channel region of MESFET.

The height of Schottky and back depletion regions from y=0and y=a in linear region under illuminated condition can be obtained by substituting Eqn. (38-39) in Eqn. (11-12).

Later, an analytical model I-V model has been developed by including deep level traps and backgating under optically controlled conditions. Using the assumption of a uniform doping profile and a gradual channel approximation with the depletion region forming at channel-substrate junction, drain-source current in linear region can be expressed as [21]:

$$I_{pv} = qZ\left(N_d - N_{sub}^{-}\right)\xi_x \left(a - h_{bg}^{f}(x) - h_{bg}^{b}(x)\right) \quad -(41)$$

Where $\xi_x = -\frac{dV}{dx}$ is electric field along the x-direction in the channel and last term represents the effective channel opening restricted by both depletion regions.

If the source and drain parasitic resistances are neglected, integrating Eqn (41) from x=0 to x=L yields the analytical expression for the I-V characteristics in linear region.

$$I_{ds} = \frac{Z\mu_n q(N_d - N_{sub}^-)}{L}\int_0^{V_{ds}} (a - h_{bg}^f(x) - h_{bg}^b(x))dv + I_{pc}$$

$$= A\left[3\left(\frac{V_{ds}}{V_{po}}\right) - 2\left(\frac{V_{ds} - V_{opgs} + f(V_{bg}) + V_{bi}}{V_{po}}\right)^{\frac{3}{2}} - \left(\frac{V_{bi} - V_{opgs} + f(V_{bg})}{V_{po}}\right)^{\frac{3}{2}}\right] - (42)$$

Where $A = \frac{Z\mu_n q^2 (N_d - N_{sub}^-)(N_{dep}^+)a^3}{6\varepsilon . L}$ is a constant

Equation (42) is strictly valid up to the onset of saturation when electric field in the channel reaches saturation electric field E_s at $V_{ds} = V_{sat} = \left[\left(\frac{1}{V_{opgs} - V_{th}}\right) + \left(\frac{1}{E_s L}\right)\right]^{-1}$ therefore $I_{ds\,sat}$ at the onset of velocity saturation is $I_{ds\,sat} = I_{ds}(V_{ds} = V_{sat})$.

In deriving Eqn. (41), we implicitly assumed that the channel length is constant. When MESFET is biased in saturation region depletion regions at drain end of gate extends laterally into the channel reducing the effective channel length. In a physical model, channel length modulation is the phenomenon producing finite output conductance in saturation region. The effective channel length of MESFET in saturation region is

$$L_{eff} = L - L_s - (43)$$

Here $L_s = 2.06K_d\left[\frac{\varepsilon_s (V_{ds} - V_{sat})}{a\sqrt{n_{cr} N_d}}\right]^{\frac{1}{2}}$ is the length of velocity Saturation region below gate [25], K_d is a domain parameter [25] and n_{cr} is the characteristic doping density of GaAs.

Analytical expression for I-V characteristics in saturation region is, $I_{ds} = I_{ds\,sat}(L \to L_{eff})$

$$I_{ds} = A_{eff}\left\{3\left[\frac{V_{sat}}{V_{po}}\right] - 2\left[\left(\frac{V_{sat} - V_{opgs} + f(V_{bg}) + V_{bi}}{V_{po}}\right)^{\frac{3}{2}} - \left(\frac{V_{bi} - V_{opgs} + f(V_{bg})}{V_{po}}\right)^{\frac{3}{2}}\right]\right.$$

$$\left. - 2\left[\frac{N_{sub}^-}{N_{dep}^+ + N_{sub}^-}\right]\left[\left(\frac{V_{sat} + V_{ch-s} - V_{opcs}}{V_{po}}\right)^{\frac{3}{2}} - \left(\frac{V_{ch-s} - V_{opcs}}{V_{po}}\right)^{\frac{3}{2}}\right]\right\} + I_{pc} - (44)$$

Where $A = A$:

$eff \quad L \to L$

eff

The first two terms in (44) are similar to the conventional analytical I-V model with gradual channel approximation and abrupt depletion layer [21]. Reduction in the drain current due to back depletion region which in turn due to the presence of deep level traps in the substrate is evident from the last term of (43). Backgating further reduces drain current by increasing the width of both depletion regions. Finally intrinsic small signal parameters like transconductance and output conductance of GaAs MESFET can be derived from the modeled I-V characteristics.

Tran conductance and drain-source resistance under illuminated conditions are

$$g_m = \frac{\partial I_{ds}}{\partial V_{gs}} :_{V_{ds}=\text{const}} \quad \text{and} \quad R_{ds} = \frac{\partial V_{ds}}{\partial I_{ds}} :_{V_{gs}=\text{const}} \qquad -(45)$$

III. RESULTS AND DISCUSSION

Photo-induced voltage across Schottky junction is presented in Fig 2(a) (dashed line) as a function of incident optical power with the device parameters in [7, 9]. The gate metal is assumed to be a semi transparent one with R_m and R_s as 0.65 and 0.2 respectively. The values of $N_{EL2,} = 1X10^{22}\ m^{-3}$ $N_{SA} = 1.1X10^{21}\ m^{-3}$, $N_{EL2,} = 1X10^{20}\ m^{-3}$, $\sigma_n = 1X10^{-18}\ m^2$ and $\sigma_p = 3X10^{-18}\ m^2$.[18]

It is observed that in fig 2(a) the external photo voltage increased with increased in incident optical power of 0.3mW is approximately 0.345V,which is closed to experimental value0.35V[9]

Variation of internal photo voltage as a function of incident optical power with the device parameters in [7, 24] is also shown in Fig 2 (a) (solid line) along with the experimental results of [24]. The value of reverse saturation current density at channel-substrate junction was estimated from [24]. It is observed that the nature is very much similar to that of external photo voltage. Larger photo absorption region in the substrate and a small reverse saturation current at channel-substrate junction makes internal photo voltage larger than external photo voltage for a given input power. The variation of photoconductive current with input optical power is depicted in Fig.2 (b) for $V_{ds} = 3.5V$ and $V_{gs} = -1V$

Various parameters used in this calculation are taken from [7]. As the input power increases, depletion widths of both front and back depletion regions decrease resulting in larger photoconductive current. Photoconductive current is typically in micro-sub micro ampere range as evident from Fig 2 (b).

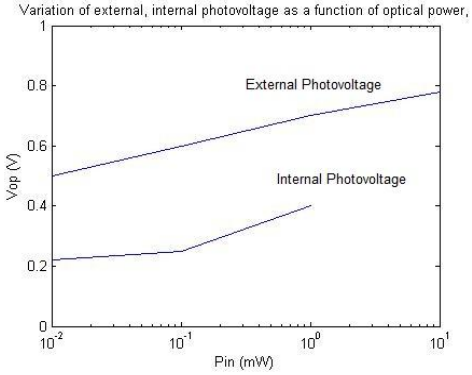

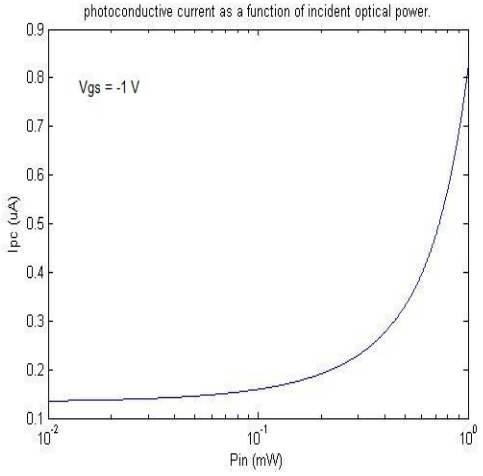

Fig. 2. Variation of (a) external, internal photo voltage as a function of optical power, (b) Photoconductive current as a function of incident Optical power.

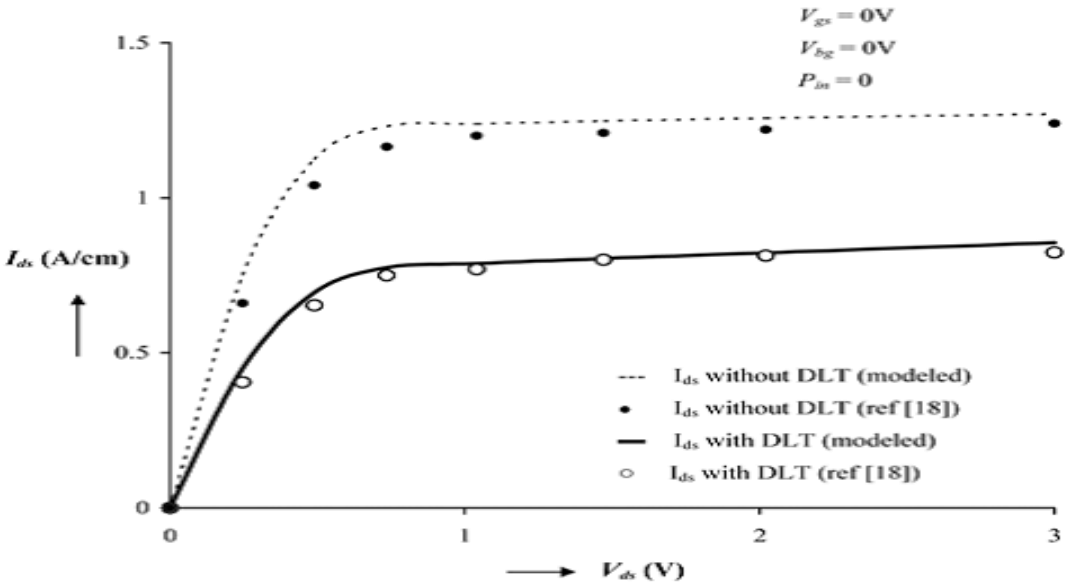

Fig. 3. Ids-Vds characteristics of Gaas MESFET without including DLT (dashed line) and Including DLT with a concentration of NEL2 = 1x1022 m-3 (solid line).

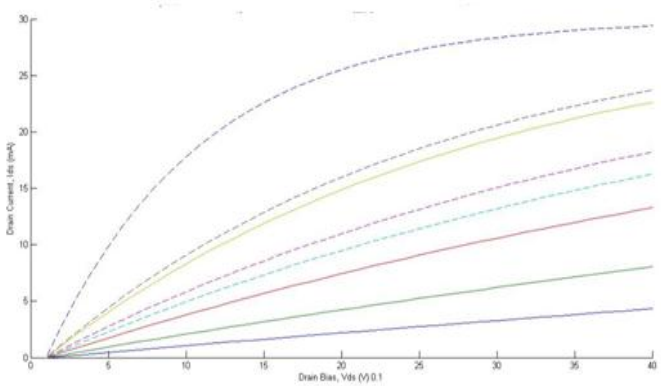

Fig.4. characteristics of Gaas MESFET under optically controlled and backgating conditions.
Fig.3.4.5.6 (waiting)

Since new expressions for I-V characteristics have been derived including deep level traps in the substrate and backgating with and without illumination, it is necessary to check validity of the above-modeled

I - V
expressions. To show how deep level traps in the substrate affect channel current, we simulated ds ds

V = 0V
characteristics without DLT (Deep Level Traps) and with DLT for gs under dark condition and are shown in Fig 3. We validated our model with the results of numerical simulation by Son et al. [18]. It is observed that presence of DLT with concentration 1x1022 /m3 degrades drain-source current severely. In order to investigate the effect of backgate voltage on the front depletion region,

$\alpha = -0.05$ $\alpha = 0.051$ α α
. A good matching is observed between the two results for 1 and 2 . Once 1 and 2 are extracted, front depletion width can be accordingly modified. Calculated dependence of backgate voltage on normalized drain-source current in saturation.

Drain-source current of GaAs MESFET under optically controlled conditions in both linear and saturation region is shown in Fig 4. Different parameters used in our model are taken from [7]. Modeled drain-source current closely tracks experimental results of [7] under dark and illuminated conditions particularly in saturation region of device operation. One can achieve better matching in linear region using a complicated velocity-field relationship rather than a simple two region model. Finite slope of I-V characteristics in saturation region is explained with the help of channel length modulation (previous models fail to account for the finite output conductance in saturation region). The effect of backgating on I-V characteristics under dark condition is also shown in the same figure. Backgate voltage greater than certain threshold voltage (V) modulates both
thbg
depletion regions thereby reducing the drain current. A substantial increase in drain current due to illumination is observed in Fig 4. Under illuminated condition of the device excess carriers in front and back depletion regions develop photo-voltages across these depletion regions which reduce respective depletion widths thereby increasing the drain-source current. Comparing Fig 2(b) and Fig 4, photoconductive current is much smaller than the total drain-source current by several orders of magnitude. Finally, photo effects on intrinsic small signal parameters of GaAs MESFET such as transconductance and output resistance are simulated and shown in Fig 5 along with backgating and DLT effects. It was observed again that presence of DLT in substrate reduces transconductance and increases output resistance particularly near threshold voltages. Backgate voltage further reduces transconductance and increases output resistance. But when the device is illuminated both photovoltaic and photoconductive effects increases transconductance and decreases output resistance

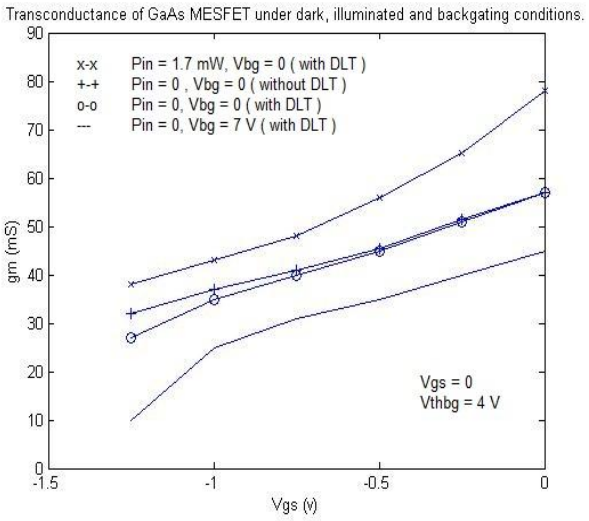

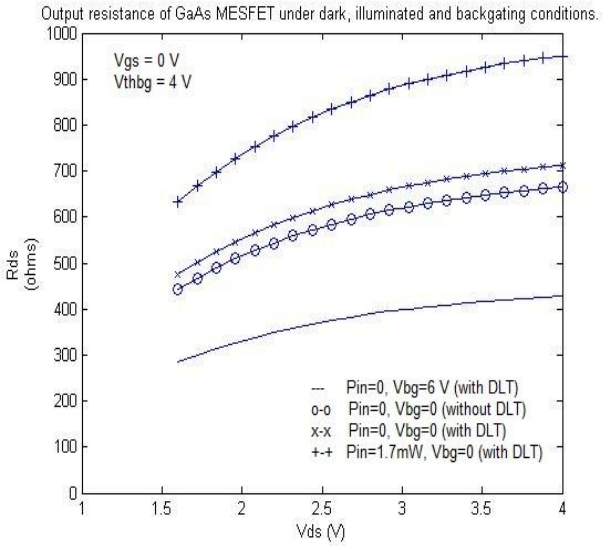

Fig. 5. Transconductance and output resistance of Gaas MESFET under dark, illuminated and backgating conditions. Deviation in transconductance and output resistance without considering DLT (ideal case), with DLT (real case) is also depicted. Various parameters in this calculation are taken from [7].

IV. CONCLUSIONS

A new and systematic way of modeling photo effects on the static I-V characteristics of GaAs MESFET's in both linear and saturation regions is presented. Effect of illumination on the device is explained in terms of photovoltaic and photoconductive effects. Photoconductive current is shown to be small by several orders of magnitude than total drain-source current. Reduction of drain-source current due to deep level traps in the substrate is explained analytically under optically controlled conditions of GaAs MESFET for the first time. Finite slope in the I-V characteristics in saturation region of GaAs MESFET is modeled with the help of channel length modulation. Further, effect of backgating is also included in modeling I-V characteristics. Finally, small signal parameters of MESFET such as transconductance and output resistance are derived from the modeled I-V characteristics. The theoretical conclusions are complemented by comparing with reported experimental results in the literature, which conform the theory. Since accurate dc modeling is key to accurate ac modeling,this model may be very useful for the designing of GaAs MESFET's particularly in MMIC's and OEIC's.

REFERENCES

[1]. A. J. Seeds, "Microwave photonics," *IEEE Trans Microwave Theory Tech*., vol. 50, no. 3, pp.877-887, March 2002.

[2]. S. J. Rossek and C.E. Free, "Optical control of microwave signals using GaAs FETs," *IEE Electron. Commun. Eng. J.*, vol.6, no. 1, pp.21-30, February 1994.

[3]. J. Rodriguez-Tellez *et al.* "Optically controlled 2.4GHz MMIC Amplifier," *Proc. of 10th International Conference on Electronics, Circuits & Systems (ICECS)*, pp.970-973, December 2003.

[4]. S. Kawasaki, H. Shiomi and K. Matsugatani, "A novel FET model including an illumination- intensity parameter for simulation of optically controlled millimeter-wave oscillators," *IEEE Trans Microwave Theory Tech*, vol. 46, no.6, pp. 820-828, June 1998.

[5]. S. Jit and B. B. Pal, "A new Optoelectronic Integrated Device for Light-Amplifying Optical Switch (LAOS)," *IEEE Trans. Electron Devices*, vol. 48, no.12, pp. 2732-2739, December 2001.

[6]. J. F. Ahadian *et al.*, "Practical OEIC's based on the monolithic integration of GaAs–InGaP LED's with commercial GaAs VLSI electronics," *IEEE J. Quantum Electron*., vol. 34, no.7, pp.1117-1123, July 1998.

[7]. A. A. De Salles, "Optical control of GaAs MESFET's," *IEEE Trans. Microwave Theory Tech.*, vol. 31, no.10, pp.812-820, October 1983.

[8]. R. N. Simons, "Microwave performance of an optically controlled AlGaAs/GaAs high electron mobility transistor and GaAs MESFET," *IEEE Trans. Microwave Theory Tech.*, vol. 35, no.12, pp.1444-1455, December 1987.

[9]. J. L. Gautier, D. Pasquet, and P. Pouvil, "Optical effects on the static and dynamic characteristics of a GaAs MESFET," *IEEE Trans. Microwave Theory Tech.*, vol.33, no.9, pp.819-822, Septem ber 1985.

[10]. [10] R. N. Simons and K. B. Bhasin, "Analysis of Optically controlled microwave/ millimeter-wave device structures," *IEEE Trans Microwave Theory Tech*, vol.34, no.12, pp.1349-1355, December 1986.
[11]. V. K. Singh and B. B. Pal, "Effect of optical radiation and surface recombination on the RF switching parameters of a GaAs MESFET," *IEE Proc. Optoelectron*., vol.137, no.2, pp. 124-128, April 1990.
[12]. P. Chakrabarti, A. Gupta, and N. A. Khan, "An analytical model of GaAs OPFET," *Solid State Electron.*, vol. 39, no.10, pp.1481-1490, October 1996.
[13]. S. H. Lo and C. P. Lee, "Numerical analysis of the photo effects in GaAs MESFET's," *IEEE Trans. Electron Devices,* vol.39, no.7, pp.1564-1570, July 1992.
[14]. N. P. Khuchua *et al.*, "Deep-Level effects in GaAs Microelectronics: A Review," *Russian Microelectronics,* vol.32, no.5, pp.257-274, 2003.
[15]. J. F. Wager and A. J. McCamant, "GaAs MESFET interface considerations," *IEEE Trans. Electron Devices,* vol. 34, no.5, pp. 1001-1007, May 1987.
[16]. F. Gao *et al.*, "Sidegating effect in ion-implanted GaAs self-aligned gate MESFET MMICs," *Proc. of GaAs Reliability workshop*, pp.27-35, Novem intensity parameter for simulation of optically controlled millimeter-wave oscillators," *IEEE Trans Microwave Theory Tech*, vol. 46, no.6, pp. 820-828, June 1998.
[17]. S. Jit and B. B. Pal, "A new Optoelectronic Integrated Device for Light-Amplifying Optical Switch (LAOS)," *IEEE Trans. Electron Devices*, vol. 48, no.12, pp. 2732-2739, December 2001.
[18]. J. F. Ahadian *et al.*, "Practical OEIC's based on the monolithic integration of GaAs–InGaP LED's with commercial GaAs VLSI electronics," *IEEE J. Quantum Electron*., vol. 34, no.7, pp.1117-1123, July 1998.
[19]. A. A. De Salles, "Optical control of GaAs MESFET's," *IEEE Trans. Microwave Theory Tech.*, vol. 31, no.10, pp.812-820, October 1983.
[20]. R. N. Simons, "Microwave performance of an optically controlled AlGaAs/GaAs high electron mobility transistor and GaAs MESFET," *IEEE Trans. Microwave Theory Tech.*, vol. 35, no.12, pp.1444-1455, December 1987.
[21]. J. L. Gautier, D. Pasquet, and P. Pouvil, "Optical effects on the static and dynamic characteristics of a GaAs MESFET," *IEEE Trans. Microwave Theory Tech.*, vol.33, no.9, pp.819-822, Septem ber 1985.
[22]. R. N. Simons and K. B. Bhasin, "Analysis of Optically controlled microwave/ millimeter-wave device structures," *IEEE Trans Microwave Theory Tech*, vol.34, no.12, pp.1349-1355, December 1986.
[23]. V. K. Singh and B. B. Pal, "Effect of optical radiation and surface recombination on the RF switching parameters of a GaAs MESFET," *IEE Proc. Optoelectron*., vol.137, no.2, pp. 124-128, April 1990.
[24]. P. Chakrabarti, A. Gupta, and N. A. Khan, "An analytical model of GaAs OPFET," *Solid State Electron.*, vol. 39, no.10, pp.1481-1490, October 1996.
[25]. S. H. Lo and C. P. Lee, "Numerical analysis of the photo effects in GaAs MESFET's," *IEEE Trans. Electron Devices,* vol.39, no.7, pp.1564-1570, July 1992.
[26]. N. P. Khuchua *et al.*, "Deep-Level effects in GaAs Microelectronics: A Review," *Russian Microelectronics,* vol.32, no.5, pp.257-274, 2003.
[27]. J. F. Wager and A. J. McCamant, "GaAs MESFET interface considerations," *IEEE Trans. Electron Devices,* vol. 34, no.5, pp. 1001-1007, May 1987.
[28]. F. Gao *et al.*, "Sidegating effect in ion-implanted GaAs self-aligned gate MESFET MMICs," *Proc. of GaAs Reliability workshop*, pp.27-35, Novem ber 1998.
[29]. E. B. Stoneham, P. A. J. O'Sullivan, S. W. Mitchell and A. F. Podell, "Working with nine different foundries", Proc. of *GaAs Integrated Circuit (GaAs IC) Symposium Tech Digest*, pp.11-14, October 1990.
[30]. I. Son and T. W. Tang, "Modeling deep-level trap effects in GaAs MESFET's," *IEEE Trans. Electron Devices*, vol. 36, no.4, pp.632-640, April 1989.
[31]. Y. H. Chen, Z. G. Wang, J. J. Qian and M. F. Sun, "Threshold behavior in backgating in GaAs metal-semiconductor field effect transistors: Induced by limitation of channel-substrate junction to leakage current," *J. Appl. Phys*., vol.81, no.1, pp.511-515, January 1997.
[32]. J. Wu, Z.G. Wang, T. W. Fan, L. Y. Lin and M. Zhang, "Sidegating effect on Schottky contact in ion-implanted GaAs," *J. Appl. Phys.*, vol. 78, no.12, pp.7422-7423, December 1995.
[33]. S. M. Sze, *Physics of Semiconductor Devices*, Wiley, New Delhi, 1999.
[34]. A. H. Khalid and A. A. Rezazadeh, "Fabrication and characterization of transparent gate field effect transistors using indium tin oxide," *IEE Proc. Optoelectron*., vol.143, no.1, pp. 7-11, February 1996.
[35]. T. Minami, "Transparent conducting oxide semiconductors for transparent electrodes," *Semicond. Sci. Technol.*, vol.20, no.4, pp. S35-S44, April 2005.
[36]. A. Madjar, P. R. Herczfeld and A. Paolella, "Analytical model for optically generated currents in GaAs MESFETs," *IEEE Trans. Microwave Theory Tech*, vol. 40, no.8, pp.1681-1691, August 1992.

[37]. Michael Shur, *GaAs Devices and Circuits*, Plenum press, New York, 1986.ber 1998.
[38]. E. B. Stoneham, P. A. J. O'Sullivan, S. W. Mitchell and A. F. Podell, "Working with nine different foundries", Proc. of *GaAs Integrated Circuit (GaAs IC) Symposium Tech Digest*, pp.11-14, October 1990.
[39]. I. Son and T. W. Tang, "Modeling deep-level trap effects in GaAs MESFET's," *IEEE Trans. Electron Devices*, vol. 36, no.4, pp.632-640, April 1989.
[40]. Y. H. Chen, Z. G. Wang, J. J. Qian and M. F. Sun, "Threshold behavior in backgating in GaAs metal-semiconductor field effect transistors: Induced by limitation of channel-substrate junction to leakage current," *J. Appl. Phys*., vol.81, no.1, pp.511-515, January 1997.
[41]. J. Wu, Z.G. Wang, T. W. Fan, L. Y. Lin and M. Zhang, "Side gating effect on Schottky contact in ion-implanted GaAs," *J. Appl. Phys.*, vol. 78, no.12, pp.7422-7423, December 1995.
[42]. S. M. Sze, *Physics of Semiconductor Devices*, Wiley, New Delhi, 1999.
[43]. A. H. Khalid and A. A. Rezazadeh, "Fabrication and characterization of transparent gate field effect transistors using indium tin oxide," *IEE Proc. Optoelectron*., vol.143, no.1, pp. 7-11, February 1996.
[44]. T. Minami, "Transparent conducting oxide semiconductors for transparent electrodes," *Semicond. Sci. Technol.*, vol.20, no.4, pp. S35-S44, April 2005.
[45]. A. Madjar, P. R. Herczfeld and A. Paolella, "Analytical model for optically generated currents in GaAs MESFETs," *IEEE Trans. Microwave Theory Tech*, vol. 40, no.8, pp.1681-1691, August 1992.
[46]. Michael Shur, *GaAs Devices and Circuits*, Plenum press, New York, 1988